15th IAPR International Conference on Machine Vision Applications (MVA)
Nagoya University, Nagoya, Japan, May 8-12, 2017.

Compressive Color Sensing Using Random Complementary Color Filter Array

Satoshi Sato[1], Nobuhiko Wakai[1], Kunio Nobori[1], Takeo Azuma[1],
Takamichi Miyata[2], Makoto Nakashizuka[2]

1. Advanced Research Division,
Panasonic Corporation
3-4 Hikaridai, Seika-cho, Soraku-gun, Kyoto
619-0237, Japan
{ sato.satoshi, wakai.nobuihiko, nobori.kunio,
azuma.takeo }@jp.panasonic.com,

2. Faculty of Engineering,
Chiba Institute of Technology
2-17-1 Tsudanuma,Narashino, Chiba
275-0016, Japan
takamichi.miyata@it-chiba.ac.jp,
nkszk@sky.it-chiba.ac.jp

Abstract

We propose a new color imaging system based on a compressive sensing technique. Our system consists of a random complementary color filter array (CFA) for random projection and a color reconstruction method for demosaicing. Our CFA overlaps two complementary color filters and consists of six color filters: cyan (C), yellow (Y), magenta (M), C+Y, C+M, and Y+M. By arranging these six color filters randomly, our imaging system achieves pseudo random projection among red (R) / green (G) / blue (B) colors, which is the key technology of compressive sensing. Because this CFA can retain more color information than RGB CFA, the proposed color reconstruction method reduces artifacts at monochromatic edges and in high-frequency regions, and obtains better image quality. As an additional contribution, we introduce saturation consistency to suppress color artifacts in saturated areas, then achieve to 3.3 dB higher quality images than the conventional method.

(a) Bayer CFA. (b) Random complementary CFA (c) Random RGB CFA.

Fig. 1. Color filter arrays.

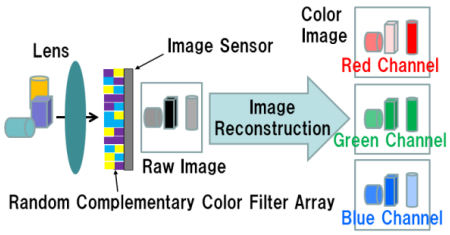

Fig. 2. Proposed color imaging system.

1. Introduction

Single-imager cameras, which use a color filter array (CFA) for color imaging, have become mainstream over the past decade. The most popular CFA is a Bayer pattern that consists of two green (G) filters, one red (R) filter, and one blue (B) filter of 2x2 pixels each, as illustrated in Fig. 1(a). In order to reconstruct a full color image from a raw image captured by this CFA, many demosaicing algorithms have been proposed. Hamilton and Adams [1] proposed Adaptive Color Plane Interpolation (ACPI) that interpolates color using the correlation among color channels and the orientation of an edge. Kiku et al. [2] proposed Minimized-Laplacian Residual Interpolation that minimizes residual Laplacian energy between the reconstructed image and the raw image. However, any demosaicing process with a Bayer CFA causes artifacts in the areas that contain monochromatic edges and/or high-frequency components, since this CFA captures only one primary color per pixel and discards the information of the other two colors.

Meanwhile, compressive sensing (CS) has recently been attracting a great deal of attention. Like the demosaicing process, the target of CS is to solve underdetermined problems. The key technology of CS is random projection [3], which is one of the optimal sampling methods. Some imaging systems with random projection have been proposed, such as Random Panchromatic CFA (RP CFA) [4], Digital Mirror Device [5], Fourier Optics [6], and Specialized Image Sensor [7]. However, these imaging systems have been impractical because they require either non-commercialized equipment or drastic changes in the design of digital cameras.

To overcome this problem, we propose a new color imaging system based on a compressive sensing technique. Our system consists of a random complementary CFA for random projection and a color reconstruction method for demosaicing. Our CFA overlaps two complementary-color filters and consists of six color filters: cyan (C), yellow (Y), magenta (M), C+Y, C+M, and Y+M. By arranging these six color filters randomly (Fig. 1(b)), our imaging system achieves pseudo random projection among R/G/B colors. Because this CFA can retain more color information than RGB CFA, the proposed method reduces artifacts at monochromatic edges and in high-frequency regions, then obtains better image quality. This idea is similar to an RP CFA [4]. The advantage of this study is that our CFA is more commercialized than an RP CFA, because our CFA needs only three color filters,

whereas an RP CFA needs numerous color filters and too many processes for fabrication.

As an additional contribution, we introduce saturation consistency [8] to reduce color artifacts which are caused by violation of an assumption for image reconstruction at saturation pixels. This technique factors the saturation phenomenon into new recovery algorithms via convex inequality constraints.

Our contributions in this study are as follows.

1. We propose a new color imaging system based on a compressive sensing technique. Our system consists of a random complementary CFA and a color reconstruction method. We achieve higher quality of reconstructed images than by RGB CFA in areas containing monochromatic edges and high-frequency components.

2. The proposed imaging system is highly practical because all that is required to implement our system is to change a Bayer CFA to a random complementary CFA, which can be achieved through minor post-processing modifications to the image sensor during fabrication.

3. Saturation consistency suppresses color artifacts in saturated areas, then leads to 3.3 dB higher quality images than the conventional method.

2. Proposed Method

In this section, we explain our proposed imaging system based on a compressive sensing (CS) technique (Fig. 2). Our color filters are randomly arranged pixel by pixel to achieve random projection among R/G/B colors. A color image is reconstructed from the captured raw image using CS technology.

2.1. Formulation of demosaicing and compressive sensing using collaborative sparsity

We explain an ideal solution for reconstructing a color image vector of size 3*N* as **x** and a given raw image vector of size *N* as **y**. A capturing process is formulated as the following equation.

$$\mathbf{y} = \mathbf{A}\mathbf{x}, \tag{1}$$

where **A** represents a sampling matrix. For a Bayer pattern CFA, the sampling matrix **A** enters one 1 for each row, while the other elements are zeros.

Demosaicing serves to solve **x** from **y**. Evidently, there are infinitely possible values for **x** because the rank of **A** < 3*N*. To obtain optimal images, CS introduces prior information that natural images have high sparsity in general. Zhang et al. [9] have formulated collaborative sparsity as the following constrained optimization problem.

$$\min_{\mathbf{x}} \left\{ \mathrm{TV}(\mathbf{x}) + \alpha \left\| \mathbf{\Theta}_{\mathbf{x}} \right\|_1 \right\} \quad \text{subject to} \quad \mathbf{y} = \mathbf{A}\mathbf{x} \tag{2}$$

where $\| \cdot \|_1$ represents L1-norm and α denotes a regularization parameter.

The former type of sparsity describes the total variation term, which is based on local two-dimensional sparsity of **x** [10, 11]. The latter one denotes non-local three-dimensional sparsity in a transform domain [12], which represents the self-similarity of natural images, while retaining the sharpness and edges effectively.

The latter sparsity is defined as follows.

1. Divide the image **x** into N_b overlapping blocks of size $N_1 \times N_1$, each block is denoted by x_k, i.e., k =1, ... , N_b.

2. Define $\mathbf{S}_{\mathbf{x}_k}$ as the set that includes the best-matching N_2 blocks to x_k in the $N_\mathrm{S} \times N_\mathrm{S}$ search window; that is, $\mathbf{S}_{\mathbf{x}_k} = \{S_{x_k \otimes 1}, S_{x_k \otimes 2}, \ldots, S_{x_k \otimes N2}\}$.

3. For every $\mathbf{S}_{\mathbf{x}_k}$, a group is formed by stacking the blocks belonging to $\mathbf{S}_{\mathbf{x}_k}$ into a three-dimensional array, which is denoted by $\mathbf{Z}_{\mathbf{x}_k}$.

4. Denote $\mathbf{T}^{3D}$ the operator of a three-dimensional transformation and $\mathbf{T}^{3D}(\mathbf{Z}_{\mathbf{x}_k})$ the transform coefficients for $\mathbf{Z}_{\mathbf{x}_k}$ in domain Ψ_{N3D} [12]. Let $\mathbf{\Theta}_{\mathbf{x}}$ be the column vector of size $K = N_1 \cdot N_1 \cdot N_\mathrm{b} \cdot N_2$ built from all of the $\mathbf{T}^{3D}(\mathbf{Z}_{\mathbf{x}_k})$ arranged in lexicographic order.

2.2. Random complementary color filter array

Random projection is known as an optimal sampling method for CS [3]. However, it has been impractical for imaging systems because it requires drastic changes in the design of digital cameras. To overcome this problem, our proposed color-imaging system introduces a random complementary CFA. General complementary CFAs consist of three color filters: C, Y, and M, which have wider bandwidths than the primary colors R, G, and B. Our color filter randomly overlaps two complementary-color filters and consists of six color filters: C, Y, M, C+Y, C+M and Y+M, as shown in Fig. 1(b). The random complementary CFA can be commercialized because it can be produced by making minor modifications to the color filter process used to fabricate image sensors.

The sampling matrix **A** for the random complementary CFA is as follows.

$$\mathbf{A} = \mathbf{B}\mathbf{C},\ \begin{bmatrix} I_C & I_Y & I_M & I_{C+Y} & I_{C+M} & I_{Y+M} \end{bmatrix}^T = \mathbf{C} \begin{bmatrix} I_R \\ I_G \\ I_B \end{bmatrix} \tag{3}$$

where **B** is a random sampling matrix that indicates the arrangement of the six-color filter, and enters one 1 for each row, while the other elements are zeros. **C** is a color conversion matrix that indicates the relationship between the six color values $I_C, I_Y, I_M, I_{C+Y}, I_{C+M}, I_{Y+M}$ and R/G/B values I_R, I_G, I_B. Because matrix **A** is the product of random sampling matrix **B** with conversion matrix **C**, it represents pseudo random projection.

Note that (1) is not always satisfied because matrix **C** that is included in **A** is a linear approximation of the process to obtain a six-color filtered image from an RGB image[a]. Therefore, we rewrite the cost function (2) as the following unconstrained optimization equation.

$$\min_{\mathbf{x}} \left\{ \frac{1}{2} \left\| \mathbf{A}\mathbf{x} - \mathbf{y} \right\|_2^2 + \tau_{\mathrm{TV}} \mathrm{TV}(\mathbf{x}) + \alpha \left\| \mathbf{\Theta}_{\mathbf{x}} \right\|_1 \right\}, \tag{4}$$

where τ_{TV} and α denote regularization parameters.

This cost function consists of three terms: a data-fidelity term, total variation term, and non-local sparsity term. The data-fidelity term is the difference between sampled reconstructed color images **x** and measurements vector **y**.

[a] We observed that, even if we use an ideal **y** and **x** (both of them is obtained from a 31-color multispectral image depicted in Fig. 3and the spectral properties shown in Fig.4), the maximum error between **Ax** and **y** reaches about 8 for 256 level (8-bit) images, because the spectral properties of the six-color filter are not obtained by a linear combination of RGB's.

2.3. Saturation consistency

In a real situation, a raw image of our system has some saturated pixels. In those pixels, the assumption of the data-fidelity term in (4) is violated, therefore the reconstructed image has severe artifacts. To overcome this problem, we introduce a technique called "saturation consistency" [8]. Because we know that the real value of a saturated pixel is larger than the measured value, we modify the optimization equation in (4) into as follows.

$$\min_{\mathbf{x}}\left\{\sum_i f_{DF}\left(\mathbf{a}_i^T\mathbf{x}, y_i\right)+\tau_{\mathrm{TV}}\mathrm{TV}(\mathbf{x})+\alpha\left\|\mathbf{\Theta}_{\mathbf{x}}\right\|_1\right\}, \quad (5)$$

where $\mathbf{a}_i$ is the transposed i-th row vector of matrix $\mathbf{A}$, y_i is the i-th element of raw image vector $\mathbf{y}$, and $f_{DF}(\cdot)$ stands for the saturation consistency operator as follows.

$$f_{DF}\left(\mathbf{a}^T{}_i\mathbf{x}, y_i\right)=\begin{cases}\frac{1}{2}\left(\mathbf{a}_i^T\mathbf{x}-y_i\right)^2 & \text{if} \quad y_i < Th_S \\ \infty & \text{if} \quad y_i \geq Th_S \text{ and } \mathbf{a}_i^T\mathbf{x} \leq Th_S, \\ 0 & \text{if} \quad y_i \geq Th_S \text{ and } \mathbf{a}_i^T\mathbf{x} > Th_S\end{cases} \quad (6)$$

where Th_S is the value of a saturated pixel. If the raw image has no saturated pixels, cost function (5) is the same as (4).

2.4. Solution of the proposed method

Although the cost function (5) is a convex problem, the optimization is not easy because none of its terms is differentiable. We apply an algorithm called the "alternating direction method of multipliers (ADMM)" [13] to solve Eq. (5) efficiently. ADMM solves the convex optimization problem by splitting it into smaller ones for variables $\mathbf{v}i$ and by partially minimizing them.

Our algorithm is shown in Table 1, where Ω_{N3D} is the inverse operator of Ψ_{N3D} (2D DCT and 1D Haar wavelet transform [12]), τ_c and μ are parameters that depend on its convergence.

Table 1. Algorithm for the proposed method.

Initialization: $\mathbf{v}_i^{(0)}=\mathbf{d}_i^{(0)}=\mathbf{0},\ i=1,2,3.\ \mathbf{p}^{(0)}=\mathbf{0}, k=0.$

Repeat:

$\mathbf{u}^{(k+1)}=\left\{\left(\mathbf{v}_1{}^{(k)}+\mathbf{d}_1{}^{(k)}\right)+\left(\mathbf{v}_2{}^{(k)}+\mathbf{d}_2{}^{(k)}\right)+\left(\mathbf{v}_3{}^{(k)}+\mathbf{d}_3{}^{(k)}\right)\right\}/3.$

If the raw image is not saturated, then

$\mathbf{v}_1{}^{(k+1)}=\left(\mathbf{A}^T\mathbf{A}+\mu\mathbf{I}\right)^{-1}\left\{\mathbf{A}^T\mathbf{y}+\mu\left(\mathbf{u}^{(k+1)}-\mathbf{d}_1{}^{(k)}\right)\right\},$

else

$\mathbf{v}_1{}^{(k+1)}=\mathbf{u}^{(k+1)}-\mathbf{d}_1{}^{(k)}+m\cdot\mathbf{a}_i,$

$$m=\begin{cases}0 & \text{if} \quad \mathbf{a}_i{}^T\left(\mathbf{u}^{(k+1)}-\mathbf{d}_1{}^{(k)}\right)\geq y_i \\ \dfrac{y_i-\mathbf{a}_i{}^T\left(\mathbf{u}^{(k+1)}-\mathbf{d}_1{}^{(k)}\right)}{\left\|\mathbf{a}_i\right\|_2^2} & else\end{cases}.$$

$$\mathbf{v}_2{}^{(k+1)}=\arg\min_{\mathbf{v}_2}\left\{\left\|\mathbf{v}_2-\mathbf{g}^{(k+1)}\right\|_2^2\Big/2\lambda+\mathrm{TV}\left(\mathbf{v}_2\right)\right\}$$

$$=\mathbf{g}^{(k+1)}-\lambda\cdot\mathrm{div}\,\mathbf{p}^{(k+1)}.$$

$\mathbf{g}^{(k+1)}=\mathbf{u}^{(k+1)}-\mathbf{d}_2^{(k)},\ \lambda=\tau_{\mathrm{TV}}/\mu$

$$\mathbf{p}_{j,i}^{(k+1)}=\frac{\mathbf{p}_{j,i}^{(k)}+\tau_c\left(\nabla\left(\mathrm{div}\mathbf{p}^{(k)}-\mathbf{g}^{(k+1)}/\lambda\right)\right)_{j,i}}{\max\left(1,\left|\mathbf{p}_{j,i}^{(k)}+\tau_c\left(\nabla\left(\mathrm{div}\mathbf{p}^{(k)}-\mathbf{g}^{(k+1)}/\lambda\right)\right)_{j,i}\right|\right)}.$$

$$\mathbf{v}_3{}^{(k+1)}=\arg\min_{\mathbf{v}_3}\left(\frac{1}{2}\left\|\mathbf{v}_3-\mathbf{r}^{(k+1)}\right\|_2^2+\frac{\alpha}{\mu}\left\|\mathbf{\Theta}_{\mathbf{v}_3}\right\|_1\right)$$

$$=\Omega_{\mathrm{N3D}}sign\left(\mathbf{\Theta}_{\mathbf{r}^{(k+1)}}\right)\min\left(\left|\mathbf{\Theta}_{\mathbf{r}^{(k+1)}}\right|-\frac{K\alpha}{N\mu},\ 0\right).$$

$\mathbf{r}^{(k+1)}=\mathbf{u}^{(k+1)}-\mathbf{d}_3{}^{(k)}.$

$\mathbf{d}_i{}^{(k+1)}=\mathbf{d}_i{}^{(k)}-\mathbf{u}^{(k+1)}-\mathbf{v}_i{}^{(k+1)},\ i=1,2,3.$

Update iteration: $k \leftarrow k+1$.

Until some stopping criterion is satisfied.

$\mathbf{x}=\mathbf{u}^{(k)}$, return ($\mathbf{x}$).

3. Experimental Results

In this section, we evaluate the performance of the proposed method.

We compared our method with the ACPI and CS reconstruction methods which use two kinds of CFAs: Bayer CFA (Fig. 1(a)) and random RGB CFA (Fig. 1(c)). The value of a saturated pixel Th_s in (6) is 255. To evaluate the performance of the proposed method, we obtain **x** and **y** using the 31-color multispectral image [14] depicted in Fig. 3 and the spectral properties of color filters shown in Fig. 4.

The simulation results for Peak-Signal-to-Noise-Ratio (PSNR) of all reconstructed images are presented in Table 2. Figure 5 depicts constructed images in the rectangular regions, which contain yellow edges and high-frequency texture in Fig. 3. These experimental results reveal the followings:

1. The images reconstructed by the ACPI and CS with the Bayer CFA have artifacts for yellow edges without saturated pixels as shown in the top row of Fig. 5. In contrast, the proposed method reconstructs a high quality image with no artifacts.

2. RGB CFAs cannot reconstruct the texture with high-frequency components, which no pixels are saturated, as shown in the bottom row of Fig. 5. In contrast, the proposed method preserves the texture and reconstructs a higher quality image than conventional images.

3. The proposed method with the saturation consistency suppresses color artifacts in saturated areas, then leads to 3.3 dB higher quality images than one without the saturation consistency.

4. Conclusion

In this study, we propose a new color imaging system based on a compressive sensing technique. Our system consists of a random complementary CFA which can be commercialized and a color reconstruction method. Our system achieves higher quality of reconstructed color images than with RGB CFA in areas containing monochromatic edges and high-frequency components.

In future work, we will evaluate real data and fabricate a prototype imaging system using the random complementary CFA. Furthermore, we will evaluate the sensitivity of our color filter because we believe that this is one of the advantages of our proposed method.

Table 2. Simulation Results.

Condition		Conventional Method			Proposed method	
	Image Reconstruction Method	ACPI	CS	CS	CS	CS
	CFA	Bayer		Random RGB	Random Complementary	
	Saturation Consistency	-	✓	✓	-	✓
PSNR [dB]	Test Image	38.23	38.41	**38.53**	35.03	38.37
	Yellow Edge Area	42.51	42.53	47.46	47.80	**48.07**
	High-frequency Texture Area	36.93	36.17	35.03	38.33	**39.56**

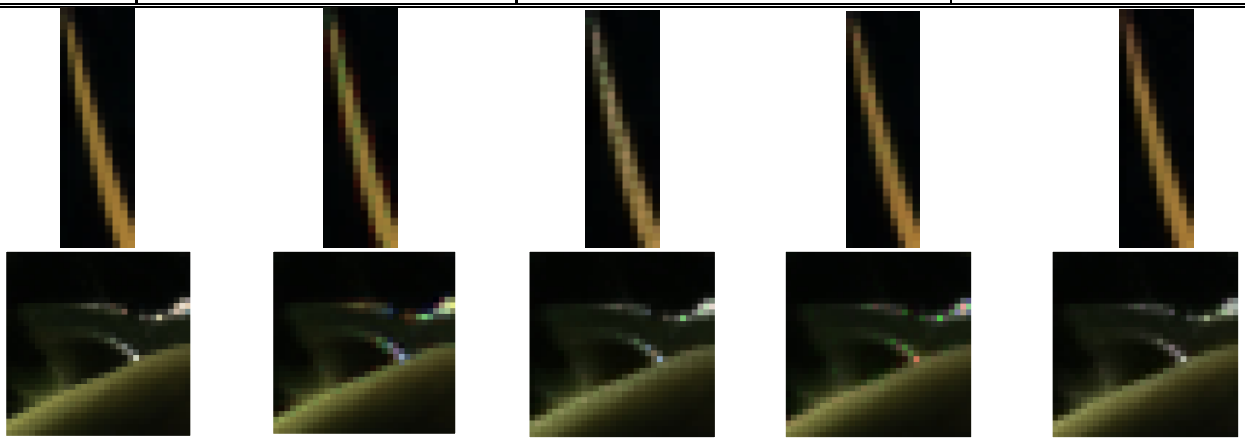

(a) Experimental test image. (b) ACPI. (c) Bayer CFA. (d) Random RGB CFA. (e) Proposed method.

Fig. 5 Reconstructed images in yellow edge and high-frequency texture areas of Fig. 3.

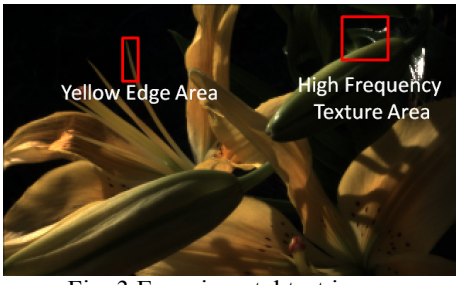

Fig. 3 Experimental test image.

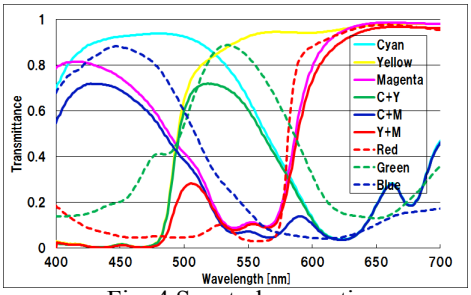

Fig. 4 Spectral properties.

References

[1] J. F. Hamilton and J. E. Adams: "Adaptive color plane in-terpolation in single sensor color electronic camera," U.S. Patent No. 5,629,734, 1997.

[2] D. Kiku et al.: "Minimized-Laplacian residual interpolation for color image demosaicking," IS&T/SPIE Electronic Imaging (EI), 2014.

[3] E. J. Candès et al.: "Robust uncertainty principles: exact signal reconstruction from highly incomplete frequency information," IEEE Trans. Inform. Theory, vol. 52, pp. 489-509, 2006.

[4] A. A. Moghadam et al.: "Compressive demosaicing," MMSP, pp. 105–110, 2010.

[5] M. Wakin et al.: "An Architecture for Compressive Imaging," ICIP, pp. 1273-1276, 2006.

[6] J. Romberg: "Compressive sensing by random convolution," SIAM Journal on Imaging Science, vol. 2, iss. 4, pp. 1098-1128, 2009.

[7] Y. Oike et al.: "A 256x256 CMOS image sensor with ΔΣ-based single-shot compressed sensing," ISSCC, 2012.

[8] J. N. Laska et al.: "Democracy in action: Quantization, saturation, and compressive sensing," Applied and Computational Harmonic Analysis, vol. 31, no. 3, pp. 429-443, 2011.

[9] J. Zhang et al.: "Image Compressive Sensing Recovery via Collaborative Sparsity," IEEE Journal on Emerging and Selected Topics in Circuits and Systems, vol.2, iss.3, pp.380-391, 2012.

[10] A. Chambolle: "An algorithm for total variation minimization and applications," Journal of Mathematical Imaging and Vision, vol. 20, pp. 89-97, 2004.

[11] S. Ono and I. Yamada: "Decorrelated vectorial total variation," CVPR, pp. 4090-4097, 2014.

[12] A. Danielyan et al.: "BM3D frames and variational image deblurring," IEEE Trans. Image Process., vol. 21, no. 4, pp. 1715-1728, 2012.

[13] D. Gabay and B. Mercier: "A dual algorithm for the solution of nonlinear variational problems via finite-element approximations," Computers & Mathematics with Applications, vol. 2, pp. 17-40, 1976.

[14] D. H. Foster et al.: "Hyperspectral images of natural scenes 2004," http://personalpages.manchester.ac.uk/staff/david.foster/Hyperspectral_images_of_natural_scenes_04.html, March 2016.